Photochemistry and Photobiology, 2002, 75(6): 627–632

DNA and Protein Changes Caused by Disease in Human Breast Tissues Probed by the Kubelka–Munk Spectral Function¶

Yuanlong Yang[1], Edward J. Celmer[2], Jason A. Koutcher[3] and R. R. Alfano*[1]

[1]Institute for Ultrafast Spectroscopy and Lasers, New York State Center for Advanced Technology for Ultrafast Photonic Materials and Applications, The City College and Graduate School of the City University of New York, New York, NY; [2]Department of Pathology, St. Vincent's Medical Center of Richmond, Staten Island, NY and [3]Memorial Sloan-Kettering Cancer Center, New York, NY

Received 4 December 2001; accepted 11 March 2002

ABSTRACT

Malignant, fibroadenoma, normal and adipose breast tissues were studied using diffuse reflectance spectroscopy. The absorption spectra of the breast tissues were extracted from the diffuse reflectance spectra using the Kubelka–Munk function (K-M function). The spectral features of the K-M function were identified and compared with those of the absorption spectra. The spectral features of the K-M function were assigned to DNA, protein, β-carotene and hemoglobin (oxygenated and deoxygenated) molecules in the breast tissue. The amplitudes of the K-M function averaged from 275 to 285 nm and from 255 to 265 nm and were found to be different for malignant, fibroadenoma and normal tissues. These differences were attributed to changes in proteins and DNA. A set of critical parameters was determined for separating malignant tissues from fibroadenoma and normal tissues. This approach should hold for other tissue types such as cervix, uterus and colon.

INTRODUCTION

Fluorescence (1–4) and excitation spectra (5,6) from native human breast tissues have been studied over the past 10 years as a potential clinical tool for purposes of cancer diagnosis. The critical parameters obtained from the intensity ratios at definite wavelengths in the fluorescence and excitation spectra have been used for separating malignant tissues from normal tissues (1–4). The differences observed in the excitation spectra have been shown to reveal changes in proteins in the cellular and extracellular matrices of malignant breast tissue (7). The changes in the excitation spectrum can be related to the degree of invasiveness of the carcinoma. These characteristics might be reflected in the absorption spectra of these tissues. Because of multiple scattering, direct measurement of absorption spectrum of tissues by conventional transmission means is not easily performed. Diffuse reflectance spectra offer a means of obtaining absorption spectra (8). Bigio and coworkers pioneered the use of the elastic scattering spectroscopy technique for measuring changes in tissue pathology (9,10). The spectra of scattered light were found to be different for different tissues. Vadium *et al.* (11) have developed polarized light scattering spectroscopy for epithelial cellular structure measurement. In these studies the reflected light was not distinguished as arising from scattering or absorption. In addition, the K-M function was not used for separating native molecular components arising from DNA, protein or fat, especially in the key spectral region between 250 and 300 nm.

Fibroadenoma, which is the most common neoplasm of the breast, is usually found in young women. It is important to distinguish fibroadenoma from malignant tumors. Until now, this may not have been possible without an invasive biopsy test.

The focus of the present paper is on using the diffuse reflectance spectrum for obtaining the K-M function of breast tissues. The spectral peaks in the K-M function revealed the content of hemoglobin (oxygenated and deoxygenated hemoglobin), collagen, β-carotene (in adipose tissue), proteins and nucleic acid (DNA) components. The amplitudes of the KMSF averaged from 275 to 285 nm and 255 to 265 nm were found to be different for malignant, fibroadenoma and normal breast tissues. These differences produced a criterion for distinguishing malignant, fibroadenoma and normal breast tissues. This approach can be applied to other tissue types such as cervix, uterus and colon.

MATERIALS

Excised normal, adipose, fibroadenoma and malignant breast tissue samples were obtained from St. Vincent's Hospital, Memorial Sloan-Kettering Cancer Center, and the National Disease Research Interchange. The size of each specimen was about 1 × 3 × 0.2 cm. Specimens were neither chemically treated nor frozen and were stored in the refrigerator for less than 24 h before optical measurements. Samples of random shapes were mounted in a 1 × 1 × 5 cm commercial quartz cuvette and were closely attached to its inner surface for measurement of spectra. Usually, the spectra were measured at up to three different locations of the sample.

A photograph of a typical specimen in a cuvette is shown in Fig.

¶Posted on the web site on 27 March 2002.

*To whom correspondence should be addressed at: Institute for Ultrafast Spectroscopy and Lasers, New York State Center for Advanced Technology for Ultrafast Photonic Materials and Applications, The City College of CUNY, 138th Street and Convent Avenue, New York, NY 10031, USA. Fax: 212-650-5530; e-mail: alfano@scisun.sci.ccny.cuny.edu

Abbreviations: K–M function, Kubelka–Munk function.

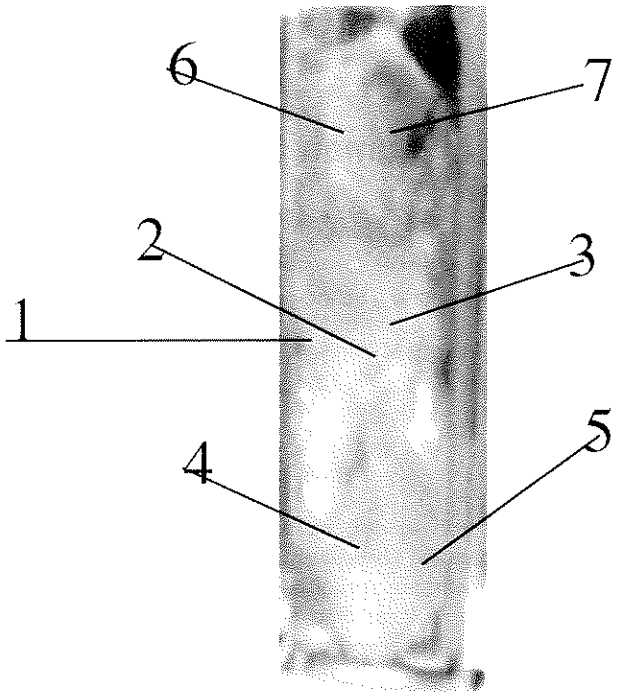

Figure 1. Photograph of a typical specimen in a cuvette. The specimen was diagnosed as a poorly differentiated carcinoma of the breast of histological grade III/III and nuclear grade III/III in the pathological report from the Memorial Sloan-Kettering Cancer Center. The diffuse reflectance method results are from locations as marked (1–7) and are given in Table 1. For comparison, the results of excitation (emission at 340 nm) and fluorescence (excited with 340 nm) methods are also given.

1. The experimental results from various locations, as marked (1–7) in Fig. 1, using the Kubelka–Munk function (K–M function) methods are displayed in Table 1. The results of the fluorescence and excitation spectrum methods are also given for comparison. More details on fluorescence and excitation methods can be found in the literature (see references 1–7). The malignant breast tissue specimens were classified as carcinoma *in situ*, infiltrating or invasive carcinoma and mixed carcinoma (part *in situ* and part invasive) according to the pathology report. Samples studied included 21 invasive carcinoma, 20 mixed carcinoma, 14 fibroadenoma, 39 normal and 30 adipose specimens. The pathological classification of these specimens is displayed in Table 2.

Table 2. Pathological classification of specimens in this experiment

Samples	Description	Total
Malignant	Ductal carcinoma	35
	Lobular carcinoma	2
	Mixed ductal and lobular carcinoma	3
	Mucinous carcinoma	1
Normal	Fibrocystic change	13
	Benign and native tissue	26
Fibroadenoma	Fibroadenoma	14
Adipose	Adipose	30

Diffuse reflectance, fluorescence and excitation spectra were obtained from the same spot of the sample using an automated dual lamp–based spectrophotometer (CD scanner, Mediscience Technology Corp., Cherry Hill, NJ). The measurements of diffuse reflectance spectra were obtained using the synchronized scan mode, in which the emission and excitation monochromators scanned the same wavelengths synchronously. The diffuse reflectance spectrum covered the range from 250 to 650 nm.

For a comparison study, a β-carotene crystal was obtained commercially from Sigma Co. (St. Louis, MO) and was dissolved in alcohol. The concentration of the carotene solution was 0.8 mg/mL. Small particles of Ti_2O_3 (0.2 μ) were added to the carotene solution for enhancing the multiscattering signal for diffuse reflectance measurements. The standard reflector Spectralon™ (Labsphere, North Sutton, NH) (R = 1) was used as a standard for the reflection measurements for all samples.

MODEL

Kubelka and coworkers (12–14) derived a basic equation for diffuse reflectance from a layer composed of absorbing and light-scattering particles that are uniformly and randomly distributed. The K–M function is given by

$$f \equiv (1 - R_\infty)^2/2R_\infty = k/s \qquad (1)$$

where $k = 2\epsilon$ and $s = 2\sigma$. The coefficient $\epsilon(k)$ is the fraction of the light absorbed per unit path length in the sample and $\sigma(s)$ is the fraction of the light that is scattered in the unit path length. R_∞ is defined as the diffuse reflectance of an infinite-thickness layer of the sample. The function f is the ratio of absorption coefficient to scattering coefficient, which

Table 1. The experimental results of K–M function, excitation and fluorescence spectra for a specimen at locations indicated in Fig. 1. The criterion for excitation spectrum is $R_1 > 1.5$, $R_2 < 1.5$ and $R_3 \geq 1$ for malignant tumor (5,6). The criterion for fluorescence spectrum for tumor is $R \geq 9$ (3,4). These three methods are consistent

	Location						
	1 (Tumor)	2 (Tumor)	3 (Tumor)	4 (Tumor)	5 (Fat)	6 (Tumor)	7 (Tumor)
K–M function							
$f(r_\infty)_{275-285\ nm}$	10.85	12.99	2.04	14.18	15.27	3.51	12.26
$f(r_\infty)_{255-265\ nm}$	14.07	30.51	1.64	31.40	38.14	3.61	13.62
$f(r_\infty)_{480\ nm}$	0.03	0.04	0.12	0.06	0.41	0.10	0.06
Excitation(emission at 340 nm)							
$R_1 = I_{289}/I_{268}$	2.04	2.08	1.75	1.89	1.85	1.91	2.00
$R_2 = I_{289}/I_{300}$	1.00	1.00	1.47	1.06	1.04	1.19	0.98
$R_3 = I_{292}/I_{283}$	1.26	1.25	1.09	1.22	1.22	1.18	1.30
Fluorescence(excited with 300 nm)							
$R = I_{340}-I_{440}$	22.39	22.78	13.01	20.25	14.66	20.49	23.31

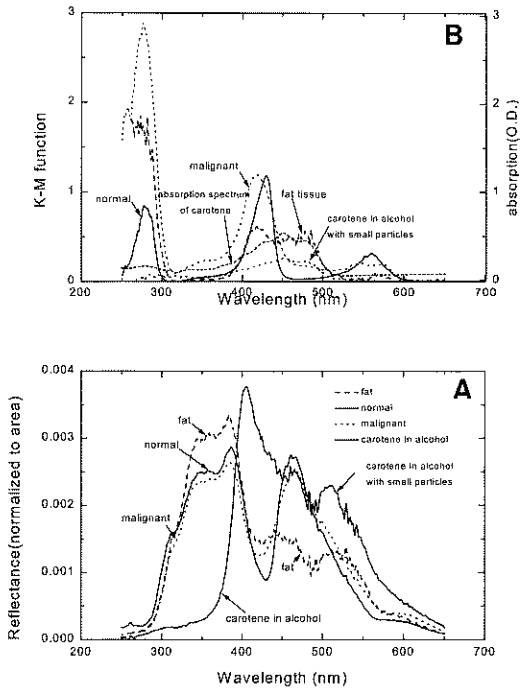

Figure 2. (a) Diffuse reflectance spectra of normal, malignant and adipose tissues and β-carotene solution. β-carotene is dissolved in alcohol. The concentration is 0.8 mg/mL. Small particles of Ti_2O_3(0.2 μ) were added to the carotene solution during diffuse reflectance measurements. To avoid the fluctuation of intensity during measurements, all the spectra have been normalized to area. For comparison, the absorption spectrum of β-carotene is included. There is no relationship connecting optical density value and the amplitude of K–M function. (b) The corresponding K–M function of the β-carotene solution, adipose, normal and malignant tissues obtained from the diffuse reflectance spectra. The absorption spectrum of a β-carotene solution determined by a transmission measurement is also presented for comparison.

is defined as the K–M function, and is frequently represented as $f(R_\infty)$.

The diffuse reflectance signal R(λ) depends on the characteristics (absorption and scattering) of the specimen and the dispersion of the instrument. A white scattering standard material with no absorption (k = 0) in the spectral region of interest was used as a reference. When this condition was fulfilled, $R_{\infty\,STD} = 1$. In our experiments, the standard scatter was certified Spectralon® 99% Reflection Standard.

Under this condition, one determines the ratio

$$r_\infty \equiv R_{\infty\,sample}/R_{\infty\,STD}. \quad (2)$$

Accordingly, r_∞ is used to calculate $f(r_\infty)$. The ratio k/s is

$$f(r_\infty) = (1 - r_\infty)^2/2r_\infty = k/s. \quad (3)$$

The scattering coefficient s smoothly changes with λ. The experimental data show that the scattering coefficient s is not significantly different between normal and malignant tissues (15). The absorption coefficient k depends on resonance. Any abrupt change in k/s is assumed to originate from the change in absorption. Assuming that $R_{\infty\,STD} = 1$ and taking the logarithm of the K–M function gives:

$$\log f(r_\infty) = \log k - \log s. \quad (4)$$

Plotting log $f(r_\infty)$ against the wavelength for a particular sample, the profile of absorption spectrum is obtained with the intercept given by $-\log s$.

Table 3. The chromophores in breast tissue from the K–M spectral structure

Chromphores	Wavelength (nm)
Hemoglobin (oxygenated)	414, 540, 578
Hemoglobin (deoxygenated)	428, 555
β-carotene	480
Collagen	340
Proteins	280
DNA	260

RESULTS

The diffuse reflectance spectra from 250 to 650 nm for several types of tissues and β-carotene are displayed in Fig. 2a. The K–M functions generated from the diffuse reflectance spectra are shown in Fig. 2b. The absorption spectrum of a β-carotene solution is also plotted in Fig. 2b for comparison. The spectral structure of the K–M functions, $f(r_\infty)$, are shown. Comparing absorption spectra of particular molecules in Table 3, the chromophores in the tissue samples were identified and are listed in Table 3.

From the experimental data, one notices that the peak of carotene at 480 nm in the K–M functions of normal and malignant tissues is not observed. The β-carotene peak only appears in adipose tissue. The averaged amplitude of the K–M function at 480 nm for different kinds of breast tissues is shown in Table 4. The adipose tissue gives a higher amplitude (0.87 ± 0.39) at 480 nm than the other tissues (0.12 ±

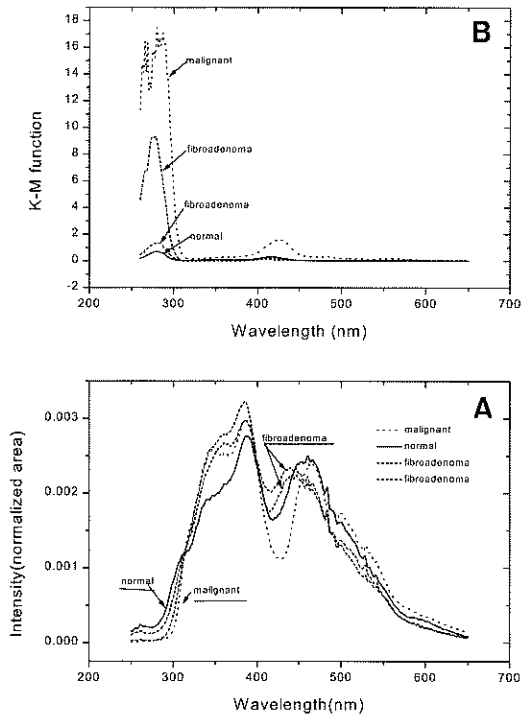

Figure 3. (a) Diffuse reflectance spectra of typical normal, fibroadenoma and malignant breast tissues. (b) Corresponding K–M function of typical normal, fibroadenoma and malignant breast tissues.

Table 4. The amplitude of the K–M function at 480 nm for different kinds of breast tissue

	Invasive	Mixed	Normal	Fibroadenoma	Adipose
$f(r_\infty)_{480\text{ nm}}$	0.22 ± 0.27	0.14 ± 0.10	0.12 ± 0.11	0.12 ± 0.09	0.87 ± 0.39

0.11 to 0.22 ± 0.27). The mean value and standard deviation of $f(r_\infty)_{480\text{ nm}}$ for adipose do not overlap with those of the other tissues.

The diffuse reflectance spectra and the K–M functions for malignant, fibroadenoma and normal breast tissues are displayed in Fig. 3a,b. The salient features found in the K–M curves of these tissues are shown in Fig. 3b and will now be discussed. The peak near 280 nm appears for all kinds of tissue, but the amplitudes are different. The amplitude of the malignant sample is higher than those of fibroadenoma and normal tissues. This peak corresponds to absorption by proteins. Another salient peak near 265 nm is prominent and appears for malignant tissue. This peak corresponds to absorption associated with DNA. For fibroadenoma the magnitude of the peak of the K–M curve near 280 nm varies, and the peak at 265 nm is not as apparent as that of malignant tissue. The amplitude of K–M at 265 nm is smaller for normal and fibroadenoma tissues.

Because of fluctuations the averaged amplitude of the K–M function from 275 to 285 nm and from 255 to 265 nm is selected as the parameter for characterizing normal, fibroadenoma and malignant (invasive carcinoma and mixed carcinoma) breast tissues. The values of the K–M function, $f(r_\infty)$, and the logarithmic K–M function, $\log f(r_\infty)$, averaged from 275 to 285 nm and from 255 to 265 nm for various tissues are shown in Table 5. The values of $f(r_\infty)_{275\text{–}285\text{ nm}}$ and $f(r_\infty)_{255\text{–}265\text{ nm}}$ were higher for malignant tissue than for normal tissue. The averaged value of $f(r_\infty)_{275\text{–}285\text{ nm}}$ is 13.11 ± 10.39 for invasive carcinoma and 0.88 ± 0.69 for normal tissue, between 275 and 285 nm. The value of the ratio $(f[r_\infty]_{275\text{–}285\text{ nm}})_{\text{invasive}}/(f[r_\infty]_{275\text{–}285\text{ nm}})_{\text{normal}}$ was found to be 14.90 and the value of $(f[r_\infty]_{275\text{–}285\text{ nm}})_{\text{mixed}}/(f[r_\infty]_{275\text{–}285\text{ nm}})_{\text{normal}}$ was found to be 5.94. The difference in $f(r_\infty)_{275\text{–}285\text{ nm}}$ for these different tissues is distinct. Nearly the same ratios were obtained for $f(r_\infty)_{255\text{–}265\text{ nm}}$. These parameters could be used as a criterion for separating normal tissue from malignant tissue but fail to separate fibroadenoma from malignant tissue. The averaged values of $f(r_\infty)_{275\text{–}285\text{ nm}}$ and $f(r_\infty)_{255\text{–}265\text{ nm}}$ for fibroadenoma are 5.23 ± 5.69 and 3.62 ± 4.41, respectively. These are higher values than for normal tissue.

A ratio parameter $A \equiv (f[r_\infty]_{275\text{–}285\text{ nm}})/(f[r_\infty]_{255\text{–}265\text{ nm}})$ is selected for separating malignant tissue from fibroadenoma. From Table 5, it is apparent that the averaged amplitude of $f(r_\infty)_{255\text{–}265\text{ nm}}$ is higher than for $f(r_\infty)_{275\text{–}285\text{ nm}}$ for malignant tissue and lower than for $f(r_\infty)_{275\text{–}285\text{ nm}}$ for normal and fibroadenoma tissues. The histogram of parameter A for malignant and fibroadenoma tissues is displayed in Fig. 4. From the histogram, one finds that the malignant tissues (invasive carcinoma and mixed carcinoma) have nearly the same distribution and peak position of the Gaussian fit curve. For fibroadenoma tissue the peak position of the Gaussian fit curve has a larger value than for malignant tissue. The statistical averaged values, standard deviations and peak position of the Gaussian fit curves of parameter A are given in Table 6. To explore the statistical meaning of the difference in parameter A between malignant and fibroadenoma tissues, a *t*-test calculation has been made, and the results are given in Table 7. The *P* value is found to be near zero for either the group of invasive carcinoma and fibroadenoma or for the group of mixed carcinoma and fibroadenoma. The difference in parameter A between these two groups is significant. Consequently, breast malignancy (invasive carcinoma and mixed carcinoma) can be distinguished from fibroadenoma.

To show the effect of the parameter A, the two-dimensional scatter figures of different kinds of tissue are plotted in Fig. 5 with $\log([\text{K–F}]_{275\text{–}285\text{ nm}})$ along the x-axis and $\log([\text{K–F}]_{255\text{–}265\text{ nm}})$ along the y-axis. The location of a specimen is related to the absorption of DNA and proteins. From Fig. 5, one can see that normal and malignant breast tissues can be easily separated by the line $x = 0.025$. On the left side of this line is the normal area. Most normal tissue data are located on the left side. On the right side of this line the tissue data are divided into two parts by the sloping line shown in the figure. Above the sloping line is the malignant area and below it is the fibroadenoma area. Thus, each kind of specimen has its own region on this special coordinate system.

The interpretation of the different regions shown in Fig. 5 is as follows: for normal tissue the absorption of proteins and DNA are lower; for malignant tissues the protein absorption is higher and DNA absorption is apparent; and for fibroadenoma tissue, sometimes, the protein absorption is as high as that of malignant tissue, but relatively smaller DNA absorption is found. Together with the change of absorption

Table 5. The averaged value of the K–M function $f(r_\infty)$ and the logarithmic K–M function ($\log f[r_\infty]$) from 275 to 285 nm and 255 to 265 nm for different kinds of breast tissue

Type of specimens	Averaged from 275 to 285 nm		Averaged from 255 to 265 nm	
	$f(r_\infty)$	$\log f(r_\infty)$	$f(r_\infty)$	$\log f(r_\infty)$
Invasive carcinoma	13.11 ± 10.39	0.98 ± 0.39	19.05 ± 18.70	1.06 ± 0.52
Mixed invasive and *in situ*	5.23 ± 4.16	0.58 ± 0.36	8.78 ± 13.30	0.65 ± 0.50
Normal	0.88 ± 0.69	−0.15 ± 0.29	0.66 ± 0.70	−0.36 ± 0.39
Fibroadenoma	5.23 ± 5.69	0.48 ± 0.46	3.62 ± 4.41	0.24 ± 0.56

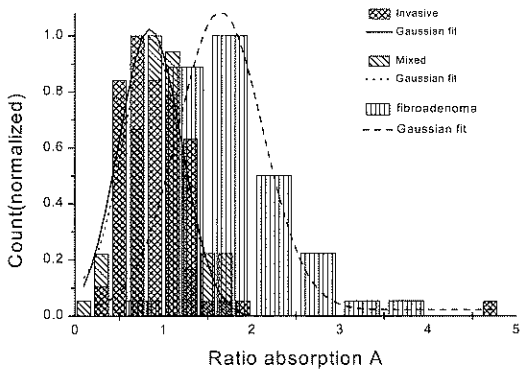

Figure 4. Histogram of invasive carcinoma, mixed carcinoma, and fibroadenoma tissues.

of DNA and proteins, malignant tissue can be separated not only from normal tissue but also from fibroadenoma. These findings are especially critical because it is important to distinguish fibroadenoma from malignancies. These observations are expected because from pathology, when a tissue changes from normal to malignant, especially locally, the DNA content is found to increase.

DISCUSSION

Table 3 displays the key chromophores in tissue using the K–M spectra. The human breast adipose tissue is bright yellow because of the accumulation of carotene in the fat cells. The K–M spectral feature at 480 nm arises from carotene. The breast is supplied with blood by vessels found in the glandular portion rather than in the fibrous and adipose stroma. The absorption peaks of the Soret band and the Q-band of hemoglobin (oxygenated and deoxygenated) in the K–M function are located at about 420 and 550 nm, respectively. The carcinoma cell *in situ* has an abundance of special proteins in the cytoplasm, and irregular nuclei. In invasive carcinoma, malignant cells invade the stroma, and changes occur in the extracellular matrix. There are qualitative and quantitative differences in the nucleic acids and proteins between normal and carcinoma invasive and mixed states. Thus a difference in the amplitude of the peaks at 260 and 280 nm in the K–M function is also found for different tissue types.

To separate the features associated with fat from those of glandular tissue is most important in the optical diagnosis of breast cancer. The key parameters from the extracted fluorescence, excitation and diffuse reflectance spectra that distinguish malignant tissue from normal tissue can be perturbed by the parameters of adipose tissue. For instance, in the fluorescence spectrum of breast tissue excited with 300 nm, the intensity ratio I_{340}–I_{440} = 9 is used as a critical value for separating malignant tissue from normal tissue (1,2). However, the intensity ratio of adipose is equal to 10, which is nearly the same as that of malignant tissue. The averaged amplitude of the K–M function $f(r_\infty)_{275-285\ nm}$ is 12.11 ± 9.23, 5.23 ± 4.16 and 0.88 ± 0.69 for invasive carcinoma, mixed carcinoma and normal tissue, respectively. For adipose tissue, it is 4.57 ± 3.74. This value overlaps with that of malignant tissue. The amplitude of the K–M function at the wavelength 480 nm, denoted by $f(r_\infty)_{480}$, is 0.22 ± 0.27, 0.12 ± 0.11 and 0.12 ± 0.09 for invasive carcinoma, normal and fibroadenoma tissue, respectively. For adipose tissue, f_{480} = 0.87 ± 0.39, which is several times greater than for the other tissues. Using this parameter, one can directly distinguish adipose tissue from other tissues.

The diffuse reflectance spectrum is used for obtaining the absorption peaks associated with protein (275–285 nm) and DNA (255–265 nm). According to the change in the amplitude, the malignant region can be differentiated from the normal and the fibroadenoma regions. Because UV and visible light penetrate tissues less than 1 mm thick, only the surface is probed; so an optical fiber needle is needed for probing inside the breast tissue.

Table 6. The averaged value of the parameter A = $(f[r_\infty]_{275-285\ nm})/(f[r_\infty]_{255-265\ nm})$ for different kinds of breast tissue

	A = $(f[r_\infty]_{275-285\ nm})/(f[r_\infty]_{255-265\ nm})$	
Type of specimens	Statistical mean value and standard deviation	Gaussian fit center and width
nvasive carcinoma	0.93 ± 0.52	0.85 ± 0.35
Mixed invasive and *in situ*	0.89 ± 0.36	0.85 ± 0.31
Normal	1.97 ± 1.42	1.49 ± 0.84
Fibroadenoma	1.82 ± 0.56	1.64 ± 0.48

Table 7. The result of a *t*-test calculation of Group 1 (fibroadenoma and invasive) and Group 2 (fibroadenoma and mixed)

Result	Group 1	Group 2
The difference of the mean value	0.89	0.93
95% confidence interval for the difference	0.20–1.09	0.77–1.09
t value	9.198	11.407
P value	0.000	0.000

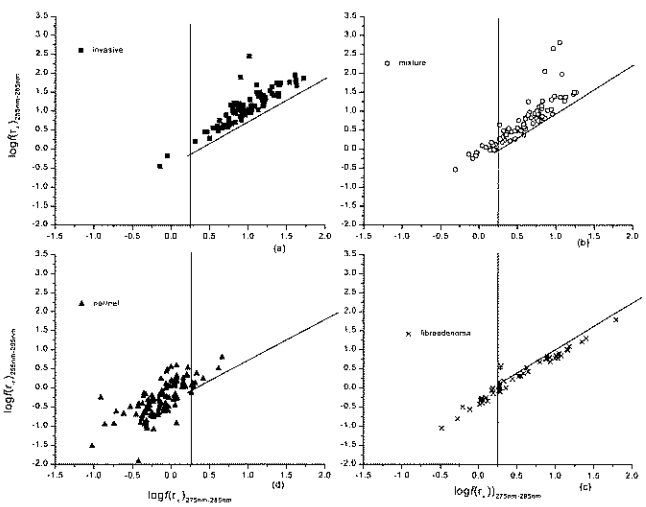

Figure 5. Two-dimensional scatter plot of invasive carcinoma (a), mixed carcinoma (b), fibroadenoma (c) and normal tissues (d) with $\log([K–F]_{275-285\ nm})$ along the *x*-axis and $\log([K–F]_{255-265\ nm})$ along the *y*-axis.

CONCLUSION

The K–F function in the UV spectral range was used to obtain the absorption peaks at 265 and 285 nm in human breast tissue. Proteins and DNA absorption peaks were observed in malignant tissues. For normal tissues the absorption of proteins and DNA was lower. Furthermore, for fibroadenoma tissue, although protein absorption was sometimes in the range found in malignant samples, relatively weaker DNA absorption was found. The K–M function gives information on DNA and protein content in tissues.

Acknowledgements—We thank Dr. N. N. Zhadin, Dr. S. Gayen, Mr. Wei Cai, Mr. Guang Zhang and Dr. N. Ockman for helpful discussions. We thank Organized Research of CUNY, Army Medical Command and DOE for support of this research, and Mediscience Technology Corp. for helping us with the CD scanner.

REFERENCES

1. Alfano, R. R., B. D. Bidyut, J. Cleary, R. Prudente and E. J. Celmer (1991) Light sheds light on cancer-distinguishing malignant tumor from benign tissue and tumors. *Bull. N.Y. Acad. Med.* **67**, 143–150.
2. Alfano, R. R., G. C. Tang, A. Pradhan and W. Lam (1987) Fluorescence spectra from cancerous and normal human breast and lung tissues. *IEEE J. Quantum Electron* **QE-23**, 1806–1811.
3. Alfano, R. R., D. B. Tata, J. Cordero, P. Tomashefsky, E. W. Longo and M. A. Alfano (1984) Laser induced fluorescence spectroscopy from native cancerous and normal tissues *IEEE J. Quantum Electron* **QE-20**, 1507–1511.
4. Yuanlong, Y., A. Katz, E. J. Celmer, M. Zarawska-Szczepaniak and R. R. Alfano (1996) Optical spectroscopy of benign and malignant breast tissue. *Lasers Life Sci.* **7**(2), 115–127.
5. Yuanlong, Y., A. Katz, E. J. Celmer, M. Zarawska-Szczepaniak and R. R. Alfano (1997) Fundamental differences of excitation spectrum between malignant and benign breast tissues. *Photochem. Photobiol.* **66**(4), 518–522.
6. Yuanlong, Y., E. J. Celmer, M. Zarawska-Szczepaniak and R R. Alfano (1997) Excitation spectrum of malignant and benign breast tissues: a potential optical biopsy approach. *Lasers Life Sci.* **7**(4), 249–265.
7. Yuanlong, Y., A. Katz, E. J. Celmer, J. A. Koutcher and R. R. Alfano (1998) Excitation spectroscopy of proteins in malignant and benign tissues. In *OSA TOPS on Biomedical Optical Spectroscopy and Diagnostics—Therapeutic Laser Application*, Vol. 22 (Edited by Eva M. Sevick-Muraca, Joseph A. Izatt and Marwood N. Ediger), pp.99–101. The Optical Society of America.
8. Zhadin, N., Y. Yang, S. Ganesan, N. Ockman and R. R. Alfano (1996) Enhancement of the fluorescence cancer diagnostic method of tissues using diffuse reflectance and the analysis of oxygenation state. *SPIE Proc.* **2697**, 142–148.
9. Bigio, J. I., J. R. Mourant, J. Boyer and T. M. Johnson (1996) Invited: Elastic scattering spectroscopy for diagnosis of tissue pathologies. In *OSA TOPS on Biomedical Optical Spectroscopy and Diagnostics*, Vol. 3 (Edited by Eva Sevick-Muraca and David Benaron), pp. 14–19. The Optical Society of America.
10. Karlheinz S., I. J. Bigio and T. R. Loree (1994) Apparatus and method for spectroscopic analysis of scattering media. U.S. Patent Number 5303026, April 12, 1994.
11. Vadium B., R. Gurjar, K. Badizadegan, I. Itzkan, R. R. Dasari, L. T. Perelman and M. S. Feld (1999) Polarized light scattering spectroscopy for quantitative measurement of epithelial cellular structures *in situ*. *IEEE J. selected Top. Quantum Electron.* **5**(4), 1019–1026.
12. Wesley, W., M. Wendlandt and H. G. Hecht (1966) *Reflectance Spectroscopy*, pp. 55–65. Interscience Publishers, New York.
13. Kubelka, P. (1948) New contribution to the optics of intensely light-scattering materials. Part I. *J. Opt. Soc. Am.* **38**(5), 448–457.
14. Kubelka, P. and F. Munk (1931) Ein beitrag zur optik der farbanstriche. *Z. Tech. Phys.* **12**, 593–604.
15. Thomsen S. and D. Tatman (1998) Physiological and pathological factors of human breast disease that can influence optical diagnosis. *Ann. N.Y. Acad. Sci.* **838**, 171–193.